Multi-electron systems in strong magnetic fields I: The 2D Landau-Hartree-Fock-Roothaan method

C. Schimeczek[a,*], G. Wunner[a]

[a]*Institut für Theoretische Physik I, Universität Stuttgart, 70550 Stuttgart, Germany*

Abstract

We present a 2-dimensional Hartree-Fock-Roothaan code to calculate wave functions and energies of light to heavy atoms in strong external magnetic fields, as they occur in the vicinity of neutron stars. The code enhances the previously presented HFFER II method, resulting in a very high precision for the energies with typical deviations less than 1% compared to the extremely precise fixed-phase diffusion quantum Monte Carlo method presented in the accompanying paper []. Despite this high precision the code is highly optimised regarding speed and reliability, which allows calculating large amounts of states in short time, even with small-scale computing clusters.

Keywords: strong magnetic field, atomic data, B-spline, Hartree-Fock-Roothaan

PROGRAM SUMMARY

Manuscript Title: Multi-electron systems in strong magnetic fields I: The 2D Landau-Hartree-Fock-Roothaan method
Authors: C. Schimeczek, G. Wunner
Program Title: 2DLHFR
Journal Reference:
Catalogue identifier:
Licensing provisions: none
Programming language: Fortran95
Computer: Cluster of 1-15 Fujitsu ESPRIMO P920
Operating system: Linux
RAM: at least 1 GByte per core

*Corresponding author.
E-mail address: Christoph.Schimeczek@itp1.uni-stuttgart.de

Number of processors used: 2-60
Keywords: strong magnetic field, atomic data, B-spline, Hartree-Fock-Roothaan
Classification: 2.1 Atomic Physics - Structure and Properties
External routines/libraries: GFortran, LAPACK, SLATEC, FMLib
Nature of problem:
The modelling of highly magnetised atmospheres of neutron stars and magnetic white dwarfs is taken for itself already a difficult task and is further complicated by the lack of atomic data. The absorption features in the thermal emission spectra of neutron stars are still not fully understood, which leads to different interpretations and thus large uncertainties for the atmospheric parameters, such as the magnetic field strength, the gravitational redshift, or the predominant atomic composition. Therefore, a fast and reliable program to scan through the large parameter space is necessary.
Solution method:
The strong magnetic fields present on neutron stars favour a wave function expansion in terms of Landau channels. Contrary to previous attempts we use a full 2-dimensional basis and assign individual z-wave functions to each Landau channel. This allows for an accurate description of the single-particle orbitals. These are combined in a Slater determinant, resulting in Hartree-Fock-Roothaan equations, which are solved iteratively. As initial wave functions we rely on the solutions calculated by the HFFER II program and reuse the optimised B-spline basis sets and Landau coefficients to maximise the speed of the program presented here.
Restrictions:
Intense magnetic field strengths $B/Z^2 \gtrsim 5 \times 10^4\,\mathrm{T}$ are required to yield accurate results.
Unusual features:
2DLHFR is based upon the wave functions calculated with the HFFER II program package, presented in [C. Schimeczek, D. Engel, G. Wunner, Comp. Phys. Comm. 183, 1502 (2012)]. In turn, the results of this program may be enhanced beyond the Hartree-Fock limit with quantum Monte Carlo methods, as is shown in the accompanying paper [].
Running time: seconds to minutes

1. Introduction

In recent years our understanding of neutron stars [1, 2] and of the relevant physical effects in the vicinity of these strongly magnetised objects [3] has increased tremendously. However, the modelling of their thermal emission spectra is still an ambitious task, mostly due to the lack of accurate data of atoms in strong magnetic fields. Unlike in the case of light elements, where highly precise line data for hydrogen (see, e.g., [4, 5, 6]) and helium (see [7, 8, 9, 10]) have been presented in the last decades, only few accurate results were published for medium-heavy or heavy atoms up to iron. If these data were available it would allow for detailed modelling of neutron star atmospheres, such as it has been reported already for magnetic white dwarfs in the literature (see, e.g., [11, 12, 13]). Up to date, the peculiar absorption features detected in isolated neutrons stars such as 1E1207.45209 [14] are discussed controversially, and are either associated with electron cyclotron harmonics [15] or oxygen and neon atomic absorptions in the atmosphere [16].

For lithium and beryllium Al-Hujaj and Schmelcher [17, 18] presented a selection of energies and transitions by means of a full configuration interaction (Full CI) method, whereas Wang and Qiao [19] contributed with Full-core-plus-correlation calculations. Heavier atoms or molecules were mainly investigated at very strong magnetic fields in adiabatic approximation (see [20, 21, 22], or at low to intermediate field strengths with a 2D Hartree-Fock method (see [23, 24]), but only up to neon. The powerful quantum Monte Carlo methods were, so far, only applied to small systems [25, 26].

In this series of papers we combine two efficient methods, namely a 2D Hartree-Fock-Roothaan approach and a fixed-phase diffusion quantum Monte Carlo method, which is known to be highly accurate. The combination of both methods has been proven to be exceedingly efficient [6] with regard to the description of atoms in strong magnetic fields, e.g. in the search of ground state electronic configurations [27]. With the Hartree-Fock method we can investigate a huge amount of states in comparatively short time, select potential ground state candidates, and then, with this selection of states, determine the true ground state configuration with very high precision using quantum Monte Carlo methods.

2. The 2D Landau-Hartree-Fock-Roothaan method

In this section we introduce the 2D Landau-Hartree-Fock-Roothaan (2DLHFR) method, which solves the problem of many-electron systems in the Coulomb potential of a nucleus with charge Z and an external magnetic field B pointing in z-direction. The strength of this field is measured by $\beta_Z = B/(Z^2 B_0)$, in units of the core-charge-scaled reference magnetic field strength $B_0 \approx 4.70103 \times 10^5\,\mathrm{T}$, where the Larmor-radius equals the Bohr-radius of the corresponding ion. We restrict ourselves to strong magnetic fields $\beta_Z \gtrsim 0.1$ and thus cylindrical coordinates are the proper choice for the non-relativistic Hamiltonian

$$\begin{aligned}\hat{H} = & \sum_{i=1}^{N} -\left(\frac{\partial^2}{\partial\rho_i^2} + \frac{1}{\rho_i}\frac{\partial}{\partial\rho_i} + \frac{1}{\rho_i^2}\frac{\partial^2}{\partial\phi_i^2} + \frac{\partial^2}{\partial z_i^2}\right) + 2\beta m_i + \beta^2\rho_i^2 \\ & + \sum_{i=1}^{N} 4\beta m_{\mathrm{s}}^i - \frac{2Z}{|\boldsymbol{r}_i|} + \sum_{\substack{i=1 \\ j=i+1}}^{N} \frac{2}{|\boldsymbol{r}_i - \boldsymbol{r}_j|}\end{aligned} \tag{1}$$

of a system with N electrons, each assigned to a magnetic quantum number m and spin z-projection m_{s}. The set of quantum numbers for each electron is completed by the z-parity π_z and an excitation number ν. We merge the latter two quantum numbers, start from zero, and obtain even excitation numbers ν for wave functions with even z-parity, and odd ν for odd z-parity wave functions. To describe a many-electron state we simply concatenate the single-particle quantum numbers and use a short notation of the form $-m^\nu$ for spin-down orbitals or $-m_\uparrow^\nu$ for spin-up orbitals.

We expand the single-particle wave functions ψ

$$\psi(\boldsymbol{r}) = \sum_{n=0}^{N_{\mathrm{L}}} P_n(z)\Phi_{nm}(\rho,\phi)\,, \tag{2}$$

as a sum of Landau orbitals Φ up to the last included Landau channel N_{L}. For each channel n, an individual z-wave function $P_n(z)$

$$P_n(z) = \sum_{\mu} \alpha_{n\mu} B_\mu(z) \tag{3}$$

is assigned, which is described by B-splines B_μ and associated coefficients $\alpha_{n\mu}$ on finite elements. We include up to $N_{\mathrm{L}} + 1 = 31$ Landau channels which

share a common B-spline decomposition per electron. In the previous code presented in Ref. [28], in the following called HFFER II, we used a product ansatz

$$\psi(\boldsymbol{r}) = \sum_{\mu} \alpha_{\mu} B_{\mu}(z) \sum_{n} t_n \Phi_{nm}(\rho, \phi)\,, \tag{4}$$

with a single longitudinal wave function $P(z)$ multiplied to a weighted sum of Landau channels using Landau weights t_n, in combination with an efficient method to optimise the B-spline node sequence of each individual electron. We use the results obtained with the HFFER II program as initial wave functions for the 2DLHFR procedure and also adopt the individual B-spline node sequences found in HFFER II for the new program.

The combination of the single-particle orbitals given in Eq. (2) in a Slater determinant and the subsequent variation of the energy functional with respect to the B-spline coefficients leads to a set of two-dimensional Hartree-Fock-Roothaan equations, i.e.

$$\sum_{n'\mu} F^i_{n\nu n'\mu} \alpha^i_{n'\mu} = \varepsilon_i \sum_{n'\mu} S^i_{n\nu n'\mu} \alpha^i_{n'\mu}\,, \tag{5}$$

where $F^i_{n\nu n'\mu}$ and $S^i_{n\nu n'\mu}$ are the Fock and overlap matrices, respectively. The Fock matrix is constructed from the sum of the longitudinal energy, transverse kinetic plus spin energy, the nuclear potential energy, as well as the direct and exchange electron-electron energy matrices, which read, in that order,

$${}^{\text{long}}F^i_{n\nu n'\mu} = -\delta_{n,n'} \int_{-\infty}^{\infty} B^i_{\nu}(z_i) \frac{\partial^2}{\partial z_i^2} B^i_{\mu}(z_i)\, \mathrm{d}z_i, \tag{6}$$

$${}^{\text{tran}}F^i_{n\nu n'\mu} = 4\beta \left(n + m^i_{\text{s}} + \frac{1}{2}\right) \delta_{n,n'} \int_{-\infty}^{\infty} B^i_{\nu}(z_i) B^i_{\mu}(z_i)\, \mathrm{d}z_i, \tag{7}$$

$${}^{\text{nucl}}F^i_{n\nu n'\mu} = \int_{-\infty}^{\infty} B^i_{\nu}(z_i) V^{nn'}_{m_i}(z_i) B^i_{\mu}(z_i)\, \mathrm{d}z_i, \tag{8}$$

$${}^{\text{dir}}F^i_{n\nu n'\mu} = \sum_{j=1}^{N} \frac{1}{\xi^j} \sum_{k,k'}^{N^j_{\text{int}}} \int_{-\infty}^{\infty} B^i_{\nu}(z_i) B^i_{\mu}(z_i) \int_{-\infty}^{\infty} P^j_k(z_j) U^{nn'kk'}_{m_i m_j}(z_i, z_j) P^j_{k'}(z_j)\, \mathrm{d}z_j\, \mathrm{d}z_i\,, \tag{9}$$

$$ {}^{\mathrm{ex}}F^{i}_{n\nu n'\mu} = -\sum_{j=1}^{N} \delta_{m_{\mathrm{s}}^{i},m_{\mathrm{s}}^{j}} \frac{1}{\xi^{j}} \sum_{k,k'}^{N_{\mathrm{int}}^{j}} \int_{-\infty}^{\infty} B^{i}_{\nu}(z_i)\, P^{j}_{k}(z_i) \int_{-\infty}^{\infty} B^{i}_{\mu}(z_j)\, A^{nn'kk'}_{m_i m_j}(z_i, z_j)\, P^{j}_{k'}(z_j)\, \mathrm{d}z_j\, \mathrm{d}z_i \,. \tag{10} $$

The two yet unknown parameters N_{int}^{j} and ξ^{j} are described in the subsequent paragraph. The overlap matrix S is defined via

$$ S^{i}_{n\nu n'\mu} = \delta_{n,n'} \int_{-\infty}^{\infty} B^{i}_{\nu}(z_i)\, B^{i}_{\mu}(z_i)\, \mathrm{d}z_i \,, \tag{11} $$

whereas the Landau-averaged potentials V, U and A used in the above formulae are given by the expressions

$$ V^{nn'}_{m_i}(z) = -2\, Z \int \frac{\Phi^{*}_{nm_i}(\boldsymbol{r}^{\perp})\, \Phi_{n'm_i}(\boldsymbol{r}^{\perp})}{|\boldsymbol{r}|}\, \mathrm{d}\boldsymbol{r}^{\perp} \,, \tag{12} $$

$$ U^{n_i n_j n'_i n'_j}_{m_i m_j}(z_i, z_j) = 2 \iint \frac{\Phi^{*}_{n_i m_i}(\boldsymbol{r}_i^{\perp}) \Phi^{*}_{n_j m_j}(\boldsymbol{r}_j^{\perp}) \Phi_{n'_i m_i}(\boldsymbol{r}_i^{\perp}) \Phi_{n'_j m_j}(\boldsymbol{r}_j^{\perp})}{|\boldsymbol{r}_i - \boldsymbol{r}_j|}\, \mathrm{d}\boldsymbol{r}_i^{\perp}\, \mathrm{d}\boldsymbol{r}_j^{\perp} \,, \tag{13} $$

$$ A^{n_i n_j n'_i n'_j}_{m_i m_j}(z_i, z_j) = 2 \iint \frac{\Phi^{*}_{n_i m_i}(\boldsymbol{r}_i^{\perp}) \Phi^{*}_{n_j m_j}(\boldsymbol{r}_j^{\perp}) \Phi_{n'_i m_i}(\boldsymbol{r}_j^{\perp}) \Phi_{n'_j m_j}(\boldsymbol{r}_i^{\perp})}{|\boldsymbol{r}_i - \boldsymbol{r}_j|}\, \mathrm{d}\boldsymbol{r}_i^{\perp}\, \mathrm{d}\boldsymbol{r}_j^{\perp} \,, \tag{14} $$

respectively. The evaluation of expressions (12), (13), and (14) is a numerically complex and costly task. Therefore, one has to precalculate all necessary effective potentials with a specialised program enclosed in the 2DLHFR program package. During the 2DLHFR runtime, the potentials are interpolated from the precalculated data sets with a six to eight digit precision, which is several magnitudes below the expected Hartree-Fock correlation error of about 1%, and allows for a fast execution of the main program.

We need to give a further explanation for the two parameters N_{int}^{j} and ξ^{j} introduced in Eqs. (9) and (10): The interaction cutoff parameter N_{int}^{j} corresponds to the highest Landau channel of electron j that we account for during the evaluation of the interaction terms in Eqs. (9) and (10). That means we evaluate the kinetic and nuclear potential matrices using the maximum number of Landau channels N_{L}, whereas we drop Landau level interaction terms between electrons i and j in both Eqs. (9) and (10) if $k, k' > N_{\mathrm{int}}^{j}$ or

$n, n' > N_{\mathrm{int}}^{i}$. Due to this disparity between the single-particle and interaction terms we induce a new cutoff error in the energy functional, lower its minimum value and deprive it of its variational nature, since the repulsive electron-electron interactions are not fully taken into account anymore. However, this loss of repulsive energy contributions can partly be compensated for with the help of renormalisation factors

$$\xi^{j} = \sum_{k=0}^{N_{\mathrm{int}}^{j}} \int_{-\infty}^{\infty} |P_{k}^{j}(z)|^{2} \, \mathrm{d}z, \tag{15}$$

which boost the interaction terms of the lower Landau channels. Such a simplification of the interaction terms is justified as long as the neglected Landau channels have small contributions to a wave function, i.e. the corresponding renormalisation factors are only marginally smaller than 1. We found renormalisation factors of $\xi < 0.95$ to cause significant deviations in the total energy, which indicates an over-simplification of the corresponding interaction terms.

This approach is physically intuitive and allows us to proceed from a rather restricted Landau expansion $N_{\mathrm{L}} = 7$ in the previous HFFER II code, to a large set of Landau channels $N_{\mathrm{L}} = 30$ in the 2DLHFR program, which gives us the possibility of an accurate description of the wave functions even at intermediately strong magnetic fields. At the same time this method economises the numerical effort needed to build the interaction matrices. If we included all interaction terms in Eqs. (9) and (10), i.e. $N_{\mathrm{int}}^{j} = N_{\mathrm{L}}$, the numerical effort would be huge since it grows proportional to $N^2 \times (N_{\mathrm{L}})^4$. Additionally, the storage of the precalculated potentials U and A would require up to 500 GB of RAM per processing unit - which is not available on any desktop computer.

2.1. Determination of the cutoff parameters

The expected sensitivity of the numerical effort on the maximum number of Landau channels considered during the calculation of interaction matrices sets the demand to find optimal cutoff parameters N_{int}^{j} for each electron in such a way that the program runtime is minimised, with only insignificant losses in the precision of the results. Since we cannot afford to repeat every calculation in search for acceptable cutoff parameters we need to find a reliable automatic method to determine reasonable cutoff parameters for each

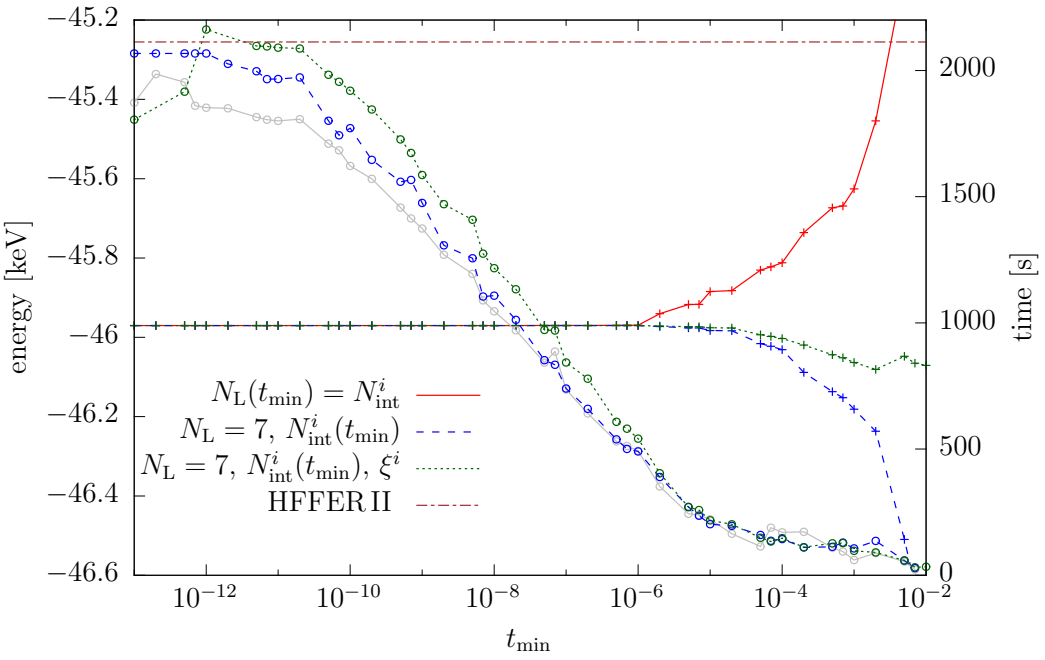

Figure 1: (Color online) Energies (crosses) and run times (circles) for the iron ground state at $B = 5 \times 10^7$ T in dependence on the minimal contribution threshold $t_{\min}$. The results were obtained using three different methods which are explained in the text. Energy results of the methods coincide up to $t_{\min} \approx 10^{-6}$. For comparison the energy result of the HFFER II program is also shown. Lines serve as a guide to the eye.

orbital. With this need in mind we analyse the Landau channel weights t^i_n of the wave functions obtained with the HFFER II method. These values represent the contributions of higher Landau channels to a set of single-particle orbitals. We define a threshold $t_{\min}$ and assume that we can ignore the interaction terms with those Landau channels whose squared contributions are below this threshold. The cutoff parameter $N^i_{\rm int}$ then corresponds to the last included Landau channel with

$$\left(t^i_{N^i_{\rm int}}\right)^2 \geq t_{\min}\,. \tag{16}$$

In order to gain a qualitative understanding of this threshold and its importance for the variation of the energy functional we show in Fig. 1 energy values and run times resulting from different $t_{\min}$. Here we restricted the overall expansion size to $N_{\rm L} = 7$. In this way we avoid an energy bias caused by neglected higher Landau channel interactions at $t_{\min} = 0$, as we can cor-

rectly include all interactions ($N_{\mathrm{int}}^i = N_{\mathrm{L}}$) in this limit. We compare three different approaches: Firstly, we reduce the Landau channel expansion number N_{L} separately for each electron according to Eq. (16) and set $N_{\mathrm{L}} = N_{\mathrm{int}}^i$. This method is still variational as it affects the single-particle and interaction terms in the same way. With increasing t_{min} we expect this to result in lower quality wave functions and thus lesser binding energies. However, up to $t_{\mathrm{min}} \approx 10^{-6}$ no significant impact on the energy values can be seen in Fig. 1 (solid curve with crosses), although we already neglect a significant amount of Landau channels. This can be seen from the enormous reduction of calculation time to about 500 s (solid curve with circles). A detailed inspection of the Landau weights reveals that the outer electrons are well described without contributions of higher Landau channels, but as soon as the inner electrons ($m' \leq 5$) are affected by the cutoff at $t_{\mathrm{min}} > 10^{-6}$ the total energy rises quickly.

In our second approach in Fig. 1 we reduce the electronic interactions using the cutoff parameters N_{int}^i (dashed curves), but keep the overall expansion of all electrons fixed at $N_{\mathrm{L}} = 7$. We omit the renormalisation factors ξ here to demonstrate the effects of the reduced interactions. As a result, the energy diverges at large t_{min}, albeit the lost variationality feigns a vast increase of the binding energy at high t_{min}. Adding the renormalisation factors ξ^i in the third approach (dotted curves) we further enhance the consistency of the energy function to variations of the cutoff parameter t_{min}, and partially compensate for the non-physical increase of the binding energy. In fact, with this approach the energy values remain quite constant up to $t_{\mathrm{min}} \approx 7 \times 10^{-4}$. A reasonable choice for t_{min}, including a safety margin, could be 10^{-6} in this calculation. In fact, hundreds of test calculations have shown that the Landau channel weights are ideally suited to determine the cutoff parameters, and the threshold of $t_{\mathrm{min}} = 10^{-6}$ has proven to work for all investigated atomic problems.

The energy functions presented in Fig. 1 were obtained using $N_{\mathrm{L}} = 7$, and we were able to double-check them in the limit $t_{\mathrm{min}} \to 0$, which effectively included all interaction terms in the calculations. To double-check the results obtained from the larger expansion using $N_{\mathrm{L}} = 30$ Landau channels we implemented a simple quantum Monte Carlo integration algorithm that is able to exactly evaluate the six-dimensional integrals of the electron-electron interactions within statistical error bounds. Note that we do not want to enhance our results beyond the Hartree-Fock limit by applying a variational or diffusion QMC method, as was done in [29, 26]. These methods work in

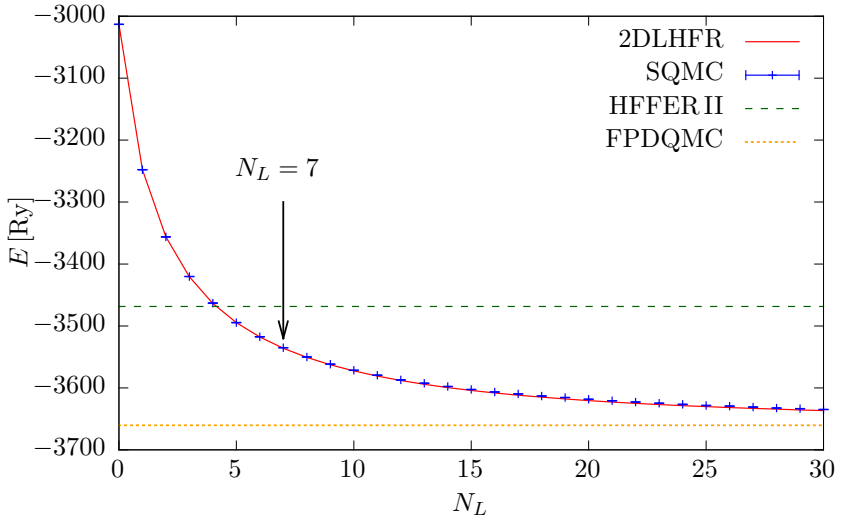

Figure 2: (Color online) Energy results for the iron ground state energy at $\beta_Z \approx 0.157$ ($B = 5 \times 10^7$ T) in dependence on the maximum Landau channel number N_L included in 2DLHFR, as well as the SQMC corrections to the energies, the corresponding FPDQMC values [6] and the HFFER II energy. Lines serve as a guide to the eye.

full configuration space, whereas we stay in the Hartree-Fock approximation and only re-evaluate the approximated two-particle integrals. Therefore, we call the method "simple quantum Monte Carlo" (SQMC) to avoid confusion with the methods presented in the accompanying paper (paper 2 []) or other works. It suffices to say that the SQMC method allows us to correctly evaluate *all* two-particle interaction terms in the energy functional as it does not rely on precalculated potentials, though it is considerably slower. Thus, we feed this method with the wave functions obtained from the variation of the slightly modified energy functional and then compute the correct energies corresponding to these modified orbitals. Figure 2 shows the energy values of the iron ground state at $\beta_Z \approx 0.157$ obtained with the 2DLHFR method at different Landau expansion sizes N_L. One can clearly see that the SQMC corrections stay very small at any N_L, while the total energy converges to a value only 0.65% above the result of the highly accurate FPDQMC method that used the 2DLHFR result as a guiding wave function. Compared with the HFFER II method we have reduced the remaining error in comparison with the FPDQMC result by a factor of 8 at $N_\mathrm{L} = 30$. If we restricted the program to the fully variational algorithm and thus to $N_\mathrm{L} = 7$, we would have reduced the error only by a factor of 1.5, as indicated by the arrow. This

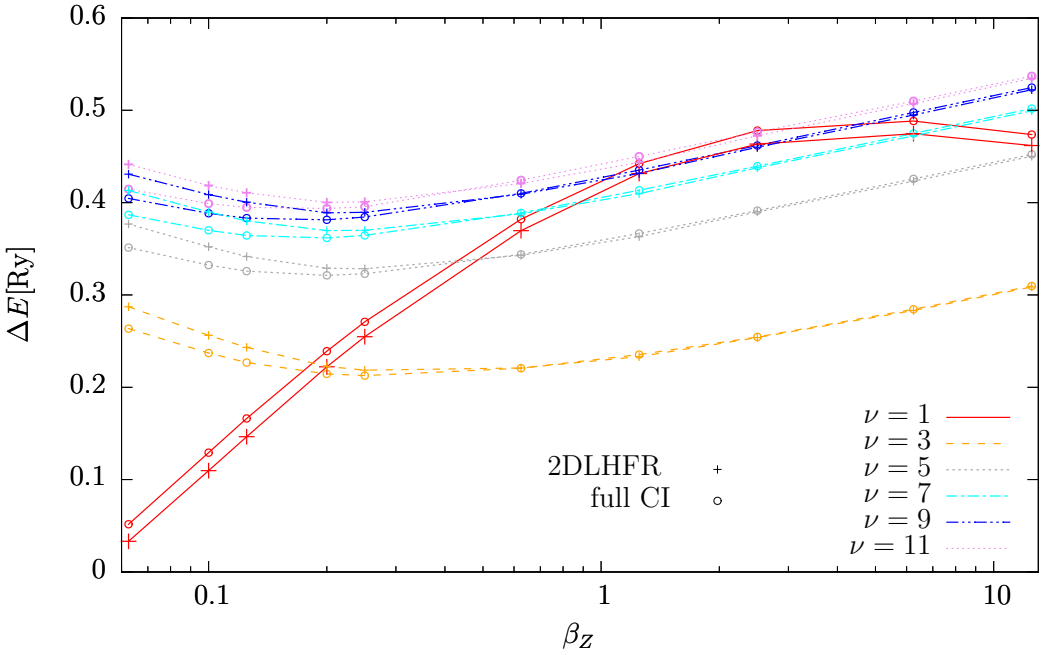

Figure 3: (Color online) Transition energies ΔE of the helium transitions from $0^0 0^2$ to $0^0 0^\nu$ over β_Z. Results from the 2DLHFR method are shown with crosses, whereas the Full CI results, taken from Becken [32], are marked with circles. Lines serve as a guide to the eye.

impressively demonstrates the power of the 2DLHFR method and justifies our approximations.

3. Results

In Ref. [6] we presented a detailed comparison of our energy results to those of other Hartree-Fock methods [30, 31], as well as to results from Full CI [7, 8, 9, 10] and fixed-phase diffusion quantum Monte Carlo calculations with the method presented in paper 2. The span of these tests included light to heavy atoms from helium to iron over the full range of the magnetic field strength accessible to the 2DLHFR program. In all investigated cases our results deviated by less than 2% from the literature values, often reaching down below 1%. However, our investigations were restricted to low-lying states only. Here, we will demonstrate that the 2DLHFR method is also suited for the calculation of higher excitations.

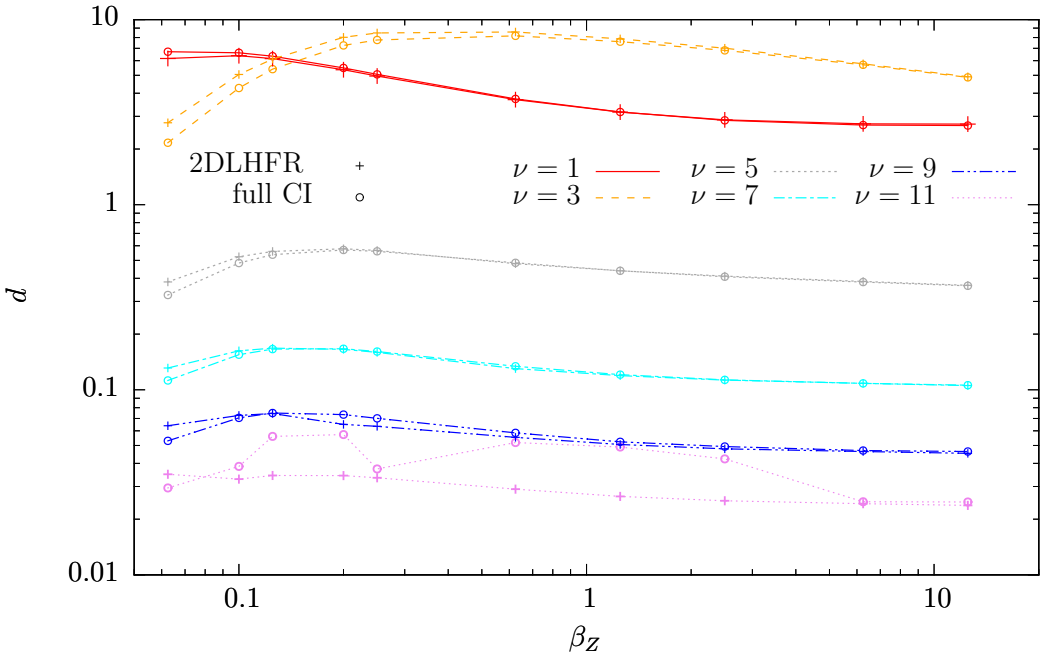

Figure 4: (Color online) Dipole strengths of the helium transitions from $0^0 0^2$ to $0^0 0^\nu$ as a function of β_Z. Results from the 2DLHFR method are shown with crosses, whereas the Full CI results, taken from Becken [32], are marked with circles. Lines serve as a guide to the eye.

In Figs. 3 and 4 we present energies and dipole strengths for the transitions from the lowest state of the helium symmetry subspace $\{M = 0,\Pi_z = +1,S_z = -1\}$ to the six lowest states of the symmetry subspace $\{M = 0,\Pi_z = -1,S_z = -1\}$, where M, Π_z and S_z denote, in that order, the total magnetic quantum number, the total z-parity and the total spin z-projection of the state. The corresponding single-particle quantum numbers are given in the caption of both figures. Also plotted are results obtained with the Full CI method of Becken [32]. The absolute line energies are small, in the range $E \leq 0.5\,\mathrm{Ry}$, since initial and final states are excited quite highly. Except for the transition to $\nu = 1$, the transition energies in Fig. 3 quickly converge to the values found with the Full CI approach. At $\beta_Z = 0.625$ the energy results of both methods agree within a relative error $< 1\%$. This also applies to the dipole strengths shown in Fig. 4, at least for the transitions to the low-lying states $\nu \leq 7$. For the highest values of ν the dipole strengths of both methods differ quite significantly for most values of the magnetic field strength. In this case the 2DLHFR dipole strength functions $d(\beta)$ retain their progression, whereas the Full CI results seem to fluctuate, especially for the transition to the highest excited state $\nu = 11$. Since Becken [32] stated to have experienced convergence problems for higher eigenvalues $\nu > 10$ and due to the smoothness of our dipole strength function $d(\beta_Z)$, we trust in the correctness of our results for the transitions to $\nu = 11$, and emphasise the high stability of the 2DLHFR method with respect to both energies and wave functions.

4. Program description

As in the previous HFFER II code, we make use of precalculated binary files, which contain all information about the effective electron-core and electron-electron potentials. The potentials are interpolated from these binary files as soon as the program starts, but require a huge amount of RAM. If one plans to use the 2DLHFR program beyond the scope of the included examples we recommend the specification of the available RAM per processing core in the `imfcon.f90` module file before one compiles the program suite to avoid RAM shortages. 2DLHFR estimates the required amount of RAM for each calculation and will fall back on a less memory-intensive but slower variant of the potential interpolation routine if necessary.

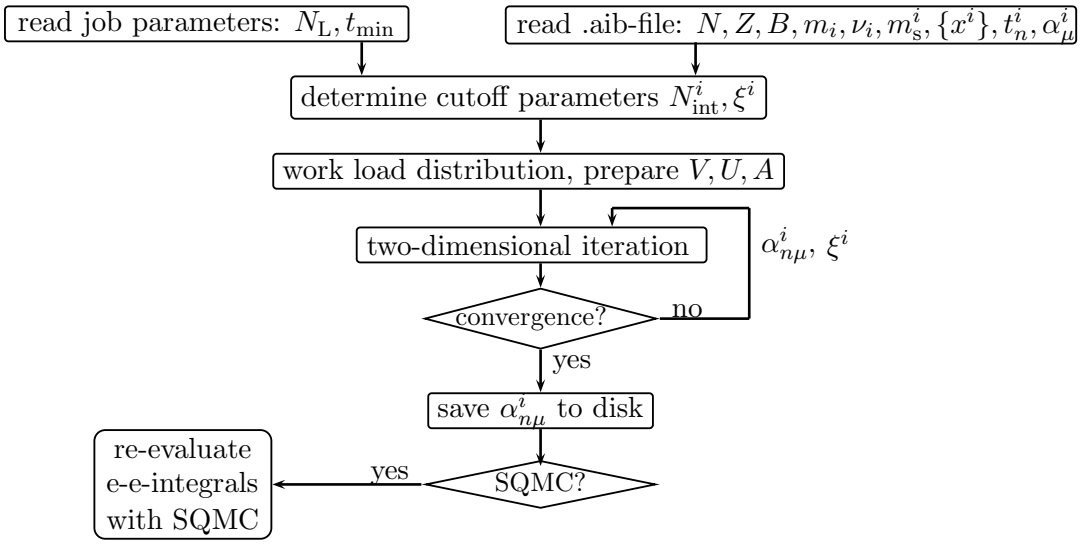

Figure 5: Scheme of the 2DLHFR program and its work flow.

4.1. Program structure and usage

The 2DLHFR program advances as depicted in Fig. 5: First, the parameter file is read. It only contains two paths: one to the working directory, where the result files are to be stored, and one to a file in `.aib` file format, resulting from HFFER II calculations. The latter file is imported as well. Additional program parameters may be adjusted using a Fortran parameter list, but this is usually not necessary. Subsequently, the cutoff parameters N_int^i for each electron i are determined from the Landau weights t_n^i, and the workload created by calculation of the interaction matrix elements is distributed among the processing cores. The main part of the program then performs the two-dimensional Hartree-Fock-Roothaan iterations and thereby optimises the B-spline coefficients $\alpha_{n\mu}^i$. The renormalisation coefficients ξ^i are also updated in each iteration step. As soon as convergence has been achieved, i.e. the total energy changes less than 10^{-3} eV between two steps, the iterations stop and the resulting wave functions and energies are written to disk in the special `.aclb` file format, which is documented in the README files. If specified, 2DLHFR can re-evaluate the interaction energies with a Monte-Carlo simulation, which is very slow but can be used to double-check the 2DLHFR energy values. This Monte-Carlo method is, again, fully parallelised via MPI.

2DLHFR uses MPI and runs best with a number of processing cores $1\times$–$2\times$ the number of electrons of the problem. Using less cores than electrons is inefficient and will result in reduced program execution speed. A suitable command to start 2DLHFR, depending on the MPI environment, is

```
mpirun -np 2 ./2dlhfr < Example1.para | tee Example1.out
```

Progression of the program is written to standard output, a sample is given below. The program package includes two additional tools: *osci* calculates transition energies and oscillator strengths for transitions of states given in the `.aclb` file format. The small tool *refiner* speeds up the evaluation of the wave function by dropping Landau channels that show negligible contributions to the single-particle energies, i.e. smaller than 10^{-3} Ry. This is important if the 2DLHFR results are used as guiding functions for consecutive simulations, such as the Monte Carlo method presented in paper 2.

Output of Example1.para

```
Starting 2DLHFR version 1.000 on   2 nodes.
READING PARAMETERS
Output directory:            ws/
Input file:                  2He0A0a_212.7171.aib
Number of electrons:                      2
Nuclear core charge:                      2
B-Spline order:                           6
Maximum Landau Level expansion:          30
Electron  1 (-m,nu,s,fem,nmax):             0  0 0  10 3
Electron  2 (-m,nu,s,fem,nmax):             0  0 1  10 3
Magn. field strength in Tesla/Beta(_Z):1.000E+008/ 212.717(  53.179)
Energy [eV] from input file:               10924.80995
Landau cut off parameter (t2prec):          1.000E-006
-----------------------------------------------
Program initialization complete.
Hartree-Fock-Roothaan iteration step:   1
-----------------------------------------
Energy of electron  1 in eV        -238.338
Energy of electron  2 in eV       11338.315
Total energy in eV              10920.44049
Iteration   1: Energy difference in eV    10920.44049

Hartree-Fock-Roothaan iteration step:   2
-----------------------------------------
Energy of electron  1 in eV        -238.261
Energy of electron  2 in eV       11338.392
Total energy in eV              10920.54047
Iteration   2: Energy difference in eV        0.09998

Hartree-Fock-Roothaan iteration step:   3
-----------------------------------------
Energy of electron  1 in eV        -238.281
Energy of electron  2 in eV       11338.372
Total energy in eV              10920.51769
Iteration   3: Energy difference in eV        0.02278
```

```
Hartree-Fock-Roothaan iteration step:   4
-----------------------------------------
Energy of electron  1 in eV        -238.278
Energy of electron  2 in eV       11338.375
Total energy in eV              10920.52091
Iteration   4: Energy difference in eV        0.00322

Hartree-Fock-Roothaan iteration step:   5
-----------------------------------------
Energy of electron  1 in eV        -238.278
Energy of electron  2 in eV       11338.374
Total energy in eV              10920.52048
Iteration   5: Energy difference in eV        0.00043

Convergence reached.
************************************************
 Beta:  212.717  Total energy:     10920.520eV
************************************************
Overall parallelization efficiency:    98.63%
```

5. Acknowledgements

[1] F. Özel, Surface emission from neutron stars and implications for the physics of their interiors, Rep. Prog. Phys. 76 (1) (2013) 016901. URL http://stacks.iop.org/0034-4885/76/i=1/a=016901

[2] J. M. Lattimer, M. Prakash, The physics of neutron stars, Science 304 (5670) (2004) 536–542. arXiv:http://www.sciencemag.org/content/304/5670/536.full.pdf, doi:10.1126/science.1090720. URL http://www.sciencemag.org/content/304/5670/536.abstract

[3] A. K. Harding, D. Lai, Physics of strongly magnetized neutron stars, Rep. Prog. Phys. 69 (9) (2006) 2631. URL http://stacks.iop.org/0034-4885/69/i=9/a=R03

[4] H. Ruder, G. Wunner, H. Herold, F. Geyer, Atoms in Strong Magnetic Fields, A&A Library, Springer-Verlag, 1994.

[5] Y. P. Kravchenko, M. A. Liberman, B. Johansson, Exact solution for a hydrogen atom in a magnetic field of arbitrary strength, Phys. Rev. A 54 (1996) 287–305. doi:10.1103/physreva.54.287.
URL http://link.aps.org/doi/10.1103/PhysRevA.54.287

[6] C. Schimeczek, S. Boblest, D. Meyer, G. Wunner, Atomic ground states in strong magnetic fields: Electron configurations and energy levels, Phys. Rev. A 88 (2013) 012509. doi:10.1103/physreva.88.012509.
URL http://link.aps.org/doi/10.1103/PhysRevA.88.012509

[7] W. Becken, P. Schmelcher, F. K. Diakonos, The helium atom in a strong magnetic field, J. Phys. B 32 (1999) 1557 – 1584. doi:10.1088/0953-4075/32/6/018.

[8] W. Becken, P. Schmelcher, Non-zero angular momentum states of the helium atom in a strong magnetic field, J. Phys. B 33 (3) (2000) 545. doi:10.1088/0953-4075/33/3/322.
URL http://stacks.iop.org/0953-4075/33/i=3/a=322

[9] W. Becken, P. Schmelcher, Higher-angular-momentum states of the helium atom in a strong magnetic field, Phys. Rev. A 63 (2001) 053412. doi:10.1103/physreva.63.053412.
URL http://link.aps.org/doi/10.1103/PhysRevA.63.053412

[10] W. Becken, P. Schmelcher, Electromagnetic transitions of the helium atom in a strong magnetic field, Phys. Rev. A 65 (2002) 033416. doi:10.1103/physreva.65.033416.
URL http://link.aps.org/doi/10.1103/PhysRevA.65.033416

[11] S. Jordan, Models of white dwarfs with high magnetic fields, A&A 265 (1992) 570–576.

[12] F. Euchner, S. Jordan, K. Beuermann, B. T. Gänsicke, F. V. Hessman, Zeeman tomography of magnetic white dwarfs, A&A 390 (2) (2002) 633–647. doi:10.1051/0004-6361:20020726.

[13] D. T. Wickramasinghe, L. Ferrario, Magnetism in isolated and binary white dwarfs, Pub. Astr. Soc. Pac. 112 (773) (2000) 873–924.
URL http://www.jstor.org/stable/10.1086/316593

[14] G. F. Bignami, A. De Luca, P. A. Caraveo, S. Mereghetti, M. Moroni, R. P. Mignani, M. Marconi, 1E1207.4-5209 - a unique object, Mem. S.A.It. 75 (3) (2004) 448.

[15] A. De Luca, R. P. Mignani, Sartori, A., Hummel, W., P. A. Caraveo, S. Mereghetti, G. F. Bignami, Hst and vlt observations of the neutron star 1e1207.45209, A&A 525 (2011) A106. doi:10.1051/0004-6361/201014982.

[16] K. Mori, C. J. Hailey, Detailed atmosphere modeling for the neutron star 1E1207.45209: Evidence of oxygen/neon atmosphere, ApJ 648 (2) (2006) 1139–1155.
URL http://stacks.iop.org/0004-637X/648/1139

[17] O. A. Al-Hujaj, P. Schmelcher, Lithium in strong magnetic fields, Phys. Rev. A 70 (3) (2004) 033411. doi:10.1103/PhysRevA.70.033411.
URL http://link.aps.org/doi/10.1103/PhysRevA.70.033411

[18] O. A. Al-Hujaj, P. Schmelcher, Beryllium in strong magnetic fields, Phys. Rev. A 70 (2) (2004) 023411. doi:10.1103/PhysRevA.70.023411.

[19] X. Wang, H. Qiao, Full-core-plus-correlation method in cylindrical coordinates: Lithium atom in strong magnetic fields, Phys. Rev. A 75 (3) (2007) 033421. doi:10.1103/PhysRevA.75.033421.
URL http://link.aps.org/doi/10.1103/PhysRevA.75.033421

[20] K. Mori, C. J. Hailey, Atomic calculation for the atmospheres of strongly magnetized neutron stars, ApJ 564 (2002) 914 – 929.

[21] Z. Medin, D. Lai, Density-functional-theory calculations of matter in strong magnetic fields. i. atoms and molecules, Phys. Rev. A 74 (6) (2006) 062507. doi:10.1103/PhysRevA.74.062507.
URL http://link.aps.org/doi/10.1103/PhysRevA.74.062507

[22] D. Engel, M. Klews, G. Wunner, A fast parallel code for calculating energies and oscillator strengths of many-electron atoms at neutron star magnetic field strengths in adiabatic approximation, Comp. Phys. Comm. 180 (2) (2009) 302 – 311. doi:doi:10.1016/j.cpc.2008.09.008.
URL http://www.sciencedirect.com/science/article/B6TJ5-4TF7CD1-1/2/39e7182bc7a40b0fc08907fc6e396c34

[23] M. V. Ivanov, P. Schmelcher, Ground state of the carbon atom in strong magnetic fields, Phys. Rev. A 60 (1999) 3558–3568.

[24] M. V. Ivanov, P. Schmelcher, Ground states of H, He,..., Ne, and their singly positive ions in strong magnetic fields: The high-field regime, Phys. Rev. A 61 (2000) 022505. doi:10.1103/PhysRevA.61.022505.
URL http://link.aps.org/doi/10.1103/PhysRevA.61.022505

[25] M. D. Jones, G. Ortiz, D. M. Ceperley, Released-phase quantum monte carlo method, Phys. Rev. E 55 (5) (1997) 6202–6210. doi:10.1103/physreve.55.6202.

[26] D. Meyer, S. Boblest, G. Wunner, Fixed-phase correlation-function quantum Monte Carlo calculations for ground and excited states of helium in neutron-star magnetic fields, Phys. Rev. A 87 (2013) 032515. doi:10.1103/PhysRevA.87.032515.
URL http://link.aps.org/doi/10.1103/PhysRevA.87.032515

[27] S. Boblest, C. Schimeczek, G. Wunner, Ground states of helium to neon and their ions in strong magnetic fields, Phys. Rev. A 89 (2014) 012505. doi:10.1103/physreva.89.012505.
URL http://link.aps.org/doi/10.1103/PhysRevA.89.012505

[28] C. Schimeczek, D. Engel, G. Wunner, A highly optimized code for calculating atomic data at neutron star magnetic field strengths using a doubly self-consistent Hartree-Fock-Roothaan method, Comp. Phys. Comm. 183 (7) (2012) 1502 – 1510. doi:10.1016/j.cpc.2012.02.011.
URL http://www.sciencedirect.com/science/article/pii/S0010465512000641

[29] S. Bücheler, D. Engel, J. Main, G. Wunner, Quantum monte carlo studies of the ground states of heavy atoms in neutron-star magnetic fields, Phys. Rev. A 76 (3) (2007) 032501. doi:10.1103/physreva.76.032501.
URL http://link.aps.org/abstract/PRA/v76/e032501

[30] M. D. Jones, G. Ortiz, D. M. Ceperley, Spectrum of neutral helium in strong magnetic fields, Phys. Rev. A 59 (4) (1999) 2875–2885. doi:10.1103/PhysRevA.59.2875.

[31] A. Thirumalai, J. S. Heyl, Hydrogen and helium atoms in strong magnetic fields, Phys. Rev. A 79 (2009) 012514.

[32] W. Becken, Elektronische struktur des helium-atoms im starken magnetfeld, Ph.D. thesis, Universität Heidelberg (2000).